ALGEBRAIC AND OPERATOR METHODS FOR GENERATION OF INFLOW DATA FOR LES AND DNS

L. di Mare
Mechanical Engineering Department,
Imperial College London
London, SW7 2AZ, UK
l.di.mare@imperial.ac.uk

W. P. Jones
Mechanical Engineering Department,
Imperial College London
London, SW7 2AZ, UK
w.jones@imperial.ac.uk

ABSTRACT

The paper describes a statistical method for the generation of inflow data for DNS and LES based on the analysis of second order two-point, two-time correlations. The method is based on the weighting of uncorrelated random numbers with appropriate coefficients, representing orthogonal decompositions of the covariance tensor itself. The novelty of the method consists in the possibility it offers of reproducing any prescribed realisable two-point, two-time correlation. To illustrate its efficacy the method is applied to the generation of inflow data starting from the two-point, two-time covariance tensor extracted from the LES of a fully developed periodic channel flow.

INTRODUCTION

The generation of accurate and realistic inflow data for LES and DNS is an area of active research and great interest because of the strong influence of inflow data on the accuracy of the computed results. Early attempts by Arnal and Friedrichs (1993) at computing flows with non-periodic boundaries were based on the use of a companion computation, the only purpose of which was to provide inflow data for the main computation. An alternative, but similar approach, based on the collection of time histories from a computation that does not require inflow data and their use as inflow data was proposed by Li et al. (2000). Even though attractive, because of the accuracy of the inflow data they generate, these techniques entail additional computational costs related to the auxiliary computation or additional storage related to the time histories. In addition in many practical flows such approaches are simply not feasible.

A different class of methods is based on the assumption, often not explicitly stated, that suitable inflow data can be constructed such that only second order statistics or a restricted set of second order statistics are reproduced. These methods make use of sequences of random number. The difficulty in this case is represented by the fact that ordinarily available random number generators only produce values that are uncorrelated, so special steps have to be taken to obtain meaningful second order statistics. The first applications of this approach appear to be those of Lee et al. (1992) and Lee et al. (1993) whereby the two-point second order correlation was prescribed in the form of an isotropic homogeneous energy spectrum, and two-time correlations were approximated by updates of the phases between the Fourier modes at random intervals. The method was also applied to the generation of inlet boundary layer data by Le et al. (1997). Klein et al. (2003) proposed the use of digital filter to provide the appropriate weights of a sequence of random numbers to reproduce Gaussian shaped two-time, two-point correlations with prescribed correlation time and length scale. In a further development of this method di Mare et al. (2005) proposed a method based on standard operations of linear algebra and the numerical solution of a bilinear difference problem to reproduce any two-time, two-point covariance.

The aim of the present paper is to propose an operator method based on the Wiener-Kintchine theorem and the use of discrete Fourier transforms, coupled with the usual tools of linear algebra, to reproduce covariance tensors. The method appears more robust than the one proposed by di Mare et al. (2005) and allows the suppression of non-realisable modes. It is also less expensive and is well suited to the treatment of very large data sets.

METHOD

This section describes the basic methods needed to reproduce any given, realisable, covariance starting from discrete sequences of uncorrelated random numbers, such as those obtained from random number generators. The discussion in this section starts from the case of a single complex variable, with the two cases of finite and infinite sets discussed separately. Finally the application of the method to two-point, two-time turbulence statistics on a plane is shown. Throughout this paper it will be assumed that the ergodic theorem applies, so that time and ensemble averages can be used interchangeably.

Finite sample size

First consider a finite set of N complex random variables f_i with prescribed covariance tensor

$$r_{ij} =< f_i f_j^* > \tag{1}$$

where $< \cdot >$ denotes ensemble averaging and $\cdot^*$ denotes the complex conjugate. The aim is to determine, if possible, a set of coefficients s_{ih} such that, given a set of uncorrelated random variables g_h with covariance tensor $< g_h g_k^* >= \delta_{hk}$, where δ_{hk} is the Kronecker symbol, the variables $q_i = s_{ih} g_h$ have covariance

$$< q_i q_j^* >= r_{ij} =< f_i f_j^* > \tag{2}$$

It can be noted immediately that

$$\begin{aligned} < s_{ih} g_h s_{jk}^* g_k^* > &= < g_h g_k^* > s_{ih} s_{jk}^* \\ &= \delta_{hk} s_{ih} s_{jk}^* \\ &= s_{ih} s_{jh}^* \end{aligned} \tag{3}$$

which shows that any symmetric factorisation s_{ih} of r_{ij} is a valid choice for the sought for coefficients. Some considerations about the existence of such a factorisation are now in order. It is to be noted that r_{ij} must be an Hermitian, positive definite matrix, as shown in Batchelor (1953). For such a matrix a symmetric factorisation is guaranteed to exist, see Golub and Loan (1996) and a legitimate choice for s_{ih} is the symmetric Cholesky factorisation of r_{ij}. This choice leads to the method proposed by Lund et al. (1998) to reproduce assigned Reynolds stresses from random data with isotropic homogeneous energy spectrum.

Another possibility is to use the fact that r_{ij} must admit a complete set of orthogonal eigenvectors, so that:

$$r_{ij} = b_{ih} \lambda_h b_{jh} \tag{4}$$

where b_{ih} are the eigenvectors of r_{ij} and λ_h are the corresponding eigenvalues. The corresponding expression for the s_{ih}s are then

$$s_{ih} = b_{ih} \sqrt{\lambda_h} \tag{5}$$

This representation of the random process f is known as its Karunen-Loeve expansion, see Loeve (1955). When the Karunen-Loeve expansion is used, the weights s_{ih} assume the physical meaning of characteristic 'eddies' of the field under consideration and have been analysed by Aubry et al. (1988) and Moin and Moser (1989). In the case of data extracted from numerical simulations or experiments, the covariance tensor r_{ij} is likely to be polluted by the presence of small negative eigenvalues. Whilst the Cholesky factorisation is likely to break down in presence of such negative eigenvalues, algorithms for the solution of the Hermitian eigen problem are stable in these conditions, so no difficulties are encountered during the computation of eigenvalues and eigenvectors of r_{ij}. Negative, non-realisable modes can be removed by writing

$$s_{ih} = b_{ih} \sqrt{max\left(\lambda_h, 0\right)} \tag{6}$$

It is worth observing that, in the case of periodic domains, the computation of eigenvectors and eigenvalues of r_{ij} reduces to a Fourier transform. This property will be made used of in the following sections. In this case, however, the immediate physical meaning of the weights s_{ih} as characteristic 'eddies' is lost, because 'eddies' are localised in space, while Fourier modes are not, see Moin and Moser (1989).

Infinite sample size

In the case of two-time correlations, the covariance tensor has the form

$$r_h =< f_i f_{i+h}^* > \tag{7}$$

with separation $h \in]-\infty; \infty[$. The weights s_i are now required to satisfy

$$r_h =< s_i g_i s_{i+h}^* g_{i+h} >= s_i s_{i+h}^* \tag{8}$$

For the purpose of the present analysis a restriction of the support of the covariance tensor to a finite size is considered, *i.e.* separations $h \in]-N/2; N/2[$ for some large value of N.

Algebraic Method. The algebraic method proposed by di Mare (2004) and di Mare et al. (2005) recognised that equation (8) defines a set of coupled bilinear difference equations with Jacobian

$$J = \begin{bmatrix} s_0 & s_1 & s_2 & \cdots & s_N \\ s_1 & s_2 & \cdots & s_N & \\ s_2 & \cdots & b_N & & \\ \vdots & & & & \\ s_N & & & & \end{bmatrix} + \begin{bmatrix} s_0 & s_1 & s_2 & \cdots & s_N \\ & s_0 & s_1 & \cdots & s_{N-1} \\ & & s_0 & \cdots & s_{N-2} \\ & & & \ddots & \vdots \\ & & & & s_0 \end{bmatrix} \tag{9}$$

It can be shown that the solution of the set of equations (8) is related to the Cholesky factorisation of a very large, symmetric matrix with band width N.

Operator Method: Fourier transforms. An alternative approach is based on the Wiener-Kintchine theorem, see Lumley (1970). The Wiener-Kintchine theorem states that if $f(t)$ is a stationary random process then there is another, unique random process $F(\omega)$ such that

$$f = \int e^{i\omega t} dF \tag{10}$$

the integral in equation (10) is a stochastic Fourier-Stiltjies integral and is presumed Lesbegue-integrable. For the purpose of the present work, the most important properties of dF are the following

$$< dF(\omega) dF^*(\omega) > = \Phi(\omega) d\omega, \quad \Phi(\omega) > 0 \tag{11}$$

$$< f(t) f^*(t+\tau) > = \int \Phi(\omega) e^{i\omega\tau} d\omega \tag{12}$$

which is a statement of the fact that the Fourier transform of the covariance of the process f is in fact the amplitude of the Fourier transform of f. Moving back to the discrete field, it is found that r_h is a covariance if and only if it has Fourier transform

$$r_h = R_k e^{-i\omega_k h} \tag{13}$$

with positive real R_k. In this case the sought for s_h are simply given by

$$s_h = \sqrt{\frac{R_k}{N}} e^{-i\omega_k h} \tag{14}$$

As noted by di Mare (2004), the numerical solution of equation (8) is very expensive and riddled with difficulty because of the nonuniqueness of its solutions and because of the possibility of introducing negative amplitudes through the restricted choice of the support. These difficulties are not encountered using equation (14), whereby non-realisable modes can be removed by writing

$$s_h = \sqrt{\frac{max\left(R_k, 0\right)}{N}} e^{-i\omega_k h} \tag{15}$$

as in the case of finite sized samples.

Two-point, two-time turbulence statistics

The application of the method to the two-point, two-time covariance tensor on the yz-plane of a turbulent channel flow is now considered. The flow is in the x direction and the y and z axis are in the wall-normal and span-wise directions respectively. The z direction is periodic. The extent of the domain in the span-wise direction is denoted by L_z and the number of nodes in this direction is N_z, while the extend of the domain in the wall-normal direction is L_y and the number of nodes is N_y. The location $y = 0$ represents the lower wall of the channel. For the purpose of the analysis that follows it is assumed that the points are equally spaced in the z direction, but no such assumption is needed in the y direction. The support of the two-time covariance will be denoted by N_t, so that separations in time $|\delta t| \leq \Delta t N_t/2 = L_t/2$, are considered, where Δt is the interval between two subsequent realisations of the flow.

The two-point, two-time covariance tensor takes the form

$$r_{ij}(y_1, y_2, \delta z, \delta t) =< f_i(y_1, z, t) f_j(y_2, z + \delta z, t + \delta t) > \quad (16)$$

where $f_i = [u', v', w', p']^\top$. A Fourier transform in z and t gives

$$r_{ij}\left(y_1, y_2, \delta z, \delta t\right) = \sum_{k_z} \sum_{k_t} R_{ij}(y_1, y_2, k_z, k_t) e^{-i(k_z \delta z + k_t \delta t)} \quad (17)$$

where $k_z = 2\pi m_z/L_z$ and $k_t = 2\pi m_t/L_t$. For the purpose of applying equation (5), the matrix R_{ij} is arranged as 4×4 block matrix with $N_y \times N_y$ entries

$$\begin{bmatrix} R_{uu} & R_{uv} & R_{uw} & R_{up} \\ R^H_{uv} & R_{vv} & R_{vw} & R_{vp} \\ R^H_{uw} & R^H_{vw} & R_{ww} & R_{wp} \\ R^H_{up} & R^H_{vp} & R^H_{wp} & R_{pp} \end{bmatrix} \quad (18)$$

where $\cdot^H$ denotes the conjugate transpose. When this partitioning for R_{ij} is chosen, the h-th eigenvector b^h_i will have the form

$$\begin{bmatrix} b^h_u \\ b^h_v \\ b^h_w \\ b^h_p \end{bmatrix} \quad (19)$$

with each $b^h_\cdot$ having N_y entries representing profiles of u, v, w and p fluctuations. The coefficients s_{ij} can now be computed as

$$s_{ih}\left(y, k_z, \delta t\right) = \sum_{k_t} b^h_i(y, k_z, k_t) \sqrt{\frac{max(\lambda_h, 0)}{N_t}} e^{-ik_t \delta_t} \quad (20)$$

where λ_h represent eigenvalues of the matrix $R_{ij}(y_1, y_2, k_z, k_t)$ corresponding to the eigenvector b^h_i. Note that equation (20) is obtained by combining equations (6) and (14). The fluctuating part of the flow field on a plane can be finally reconstructed from

$$f_i(y, z) = \sum_h \sum_{k_z} \sum_{\delta t} s_{ih}\left(y, k_z, \delta t\right) e^{-ik_z z} \phi_h\left(k_z, \delta t\right) \quad (21)$$

where $\phi_h\left(k_z, \delta t\right)$ is a set of random complex numbers with zero covariance.

RESULTS AND DISCUSSION

In this section the methods described above are applied to the generation of inflow data for a fully developed turbulent channel flow at $Re_\tau = 360$, based on channel half height δ. The reference computation is a periodic channel flow performed using a grid of $N_x N_y N_z = 96 \times 64 \times 96$ nodes. The solution domain extends over 6δ, 2δ and 3δ in the stream-wise, wall-normal and span-wise directions, respectively. The wall adjacent grid points are at a position corresponding t $y^+ = 1.5$ and the stream-wise and span-wise grid spacings are uniform with $\Delta x^+ = 20$ and $\Delta z^+ = 10$, approximately. To maintain temporal accuracy the time step Δt is adjusted to ensure $0.1 \leq CFL \leq 0.3$. To represent sub-grid stresses the Smagorinsky SGS model is applied, with Van Driest damping next to the wall. The numerical method used for the computations is based on a finite volume incompressible solver with co-located variable arrangement and implicit time stepping. The code is formally second order accurate in space and time and uses fourth order pressure smoothing to prevent decoupling of the pressure and velocity fields. Further details of the code are provided in Jones (1991); Jones and Wille (1996); di Mare and Jones (2003); di Mare (2004).

The two-point, two-time covariance tensor (16) is extracted from a database containing 20000 realisations of the flow. The size of the sample is increased four-folds by exploiting the symmetry groups $y \rightarrow -y$ and $z \rightarrow -z$. The support of the covariance in time is truncated to a separation $|\delta t| \leq 3\frac{\delta}{U_0}$, where U_0 is the bulk average velocity in the channel, which corresponds approximately to a full flow through time or 1000 time steps.

The inflow-outflow computation is performed on the same mesh and with the same numerical parameters as the periodic computation. For the inflow-outflow computation a new inflow field is generated via equation (21) at each time step. In order to do so, a new set of $\phi_h\left(k_z, \delta t\right)$ is generated for $\delta t = 3\frac{\delta}{U_0}$. All the previously generated values of ϕ are shifted in time by $-\Delta t$ and reused. For the current computations only the first 20 eigenmodes and 21 tangential modes (including $k_z = 0$) are retained. The fluctuations obtained with equation (21) are superimposed to the mean velocity profile obtained from the same database.

Figures 1 to 4 show contour plots for the real part of the matrix $R_{ij}(y_1, y_2, k_z, 0)$ for $m_z = 5$. Shown are the diagonal blocks of the matrix and the block corresponding to the uv Reynolds stress. This particular span-wise mode is active within 100 wall units from each wall. Figure 5 shows the velocity fluctuation profiles corresponding to the first eigenvector of the matrix, *i.e.* the one associated with the largest eigenvalue. The velocity profiles are also most active within 100 wall units from the wall. It can be seen that in this eigenmode stream-wise and wall-normal velocity fluctuations have different signs, so as to produce negative uv Reynolds stress. This situation is typical of other span-wise wave-numbers as well.

The accuracy of the results computed from the periodic simulation is verified by comparisons with the DNS results of by Moser et al. (1990). Figures 6, 7 and 8 show comparisons of the average stream-wise velocity profile, turbulence intensities and Reynolds stresses, respectively. The slope and intercept of the log-law and amplitude and position of the maxima in turbulence intensities and Reynolds stress are well reproduce by the periodic computation, except very close to the wall.

The agreement between the present results and the DNS results is reasonable and adequate for the purpose of the present study.

The same comparison is then performed for the flow statistics at $x = 3\delta$ downstream from the inflow of the inflow-outflow computation. The corresponding data are shown in figures 9, 10 and 11. Very little change can be seen in the mean flow profile as well as in the shape of the turbulence intensities and Reynolds stresses. A small decay in amplitude of these last quantities can be observed, which is easily explained in terms of the large number of modes of the inlet flow field discarded in the present analysis. The overall agreement between the inflow-outflow computation and the reference data is, however, satisfactory.

CONCLUSIONS

The paper has described a technique, based on standard tools of signal processing, for the generation of inflow conditions for LES and DNS starting from any realisable two-point, two-time covariance tensor. The method allows a clear distinction between the mathematical problem of reproducing covariance tensors starting from uncorrelated random numbers and the turbulence problem of prescribing realistic covariance tensors, *i.e.* realistic descriptions of the turbulence structures present in the inlet flow field. The effectiveness of the method has been illustrated by the generation of inflow data starting from the full covariance tensor extracted from the LES of a fully developed turbulent channel flow.

ACKNOWLEDGEMENTS

LdM gratefully acknowledges support from DTI and Rolls-Royce plc.

REFERENCES

*

References

Arnal, M. and Friedrichs, R. (1993). Large-Eddy simulation of a turbulent flow with separation. In *Selected papers from the eighth Symposium on Turbulent Shear Flows*, pages 169–187. Springer Verlag.

Aubry, N., Holmes, P., Lumley, J. L., and Stone, E. (1988). The dynamics of coherent structures in the wall region of a turbulent boundary layer. *Journal of Fluid Mechanics*, 192:115–173.

Batchelor, G. K. (1953). *Theory of Homogeneous Turbulence*. Cambridge University Press.

di Mare, L. (2004). *Large Eddy Simulation of wall bounded turbulent flows*. PhD thesis, Imperial College London.

di Mare, L. and Jones, W. P. (2003). LES of turbulent flow past a swept fence. *Int. J Heat and Fluid Flow*, 24:606–615.

di Mare, L., Klein, M., Jones, W. P., and Janicka, J. (2005). Synthetic turbulence inflow conditions for large eddy simulation. *submitted for publication*.

Golub, G. H. and Loan, C. F. V. (1996). *Matrix Computations*. John Hopkins University Press.

Jones, W. P. (1991). *BOFFIN: a computer program for flow and combustion in complex geometries*.

Jones, W. P. and Wille, M. (1996). Large eddy simulation of a plane jet in a cross flow. *International Journal of Heat Fluid Flow*, 37:296–306.

Klein, M., Sadiki, A., and Janicka, J. (2003). A digital filter based generator of inflow data for spatially developing direct numerical or large eddy simulations. *J. Comp. Physics*, 186:652–665.

Le, H., Moin, P., and Kim, K. (1997). Direct Numerical Simulation of turbulent flow past a backward-facing step. *Journal of Fluid Mechanics*, 330:349–374.

Lee, S., Lele, S. K., and Moin, P. (1992). Simulation of spatially evolving turbulence and the applicability of Taylor's hypothesis in compressible flows. *Physics of Fluids A*, 4(7):1521–1530.

Lee, S., Lele, S. K., and Moin, P. (1993). Direct Numerical Simulation of isotropic turbulence interacting with a wak sock wave. *Johrnal of Fluid Mechanics*, 251.

Li, N., Balaras, E., and Piomelli, U. (2000). New conditions for Large-Eddy Simulation of mixing layers. *Physics of Fluids*, 12(4):935–938.

Loeve, M. M. (1955). *Probability theory*. Van Nostrand.

Lumley, J. L. (1970). *Stochastic tools in turbulence*. Academic Press.

Lund, T. S., Wu, X., and Squires, K. D. (1998). Generation of inflow data for spatially-developing boundary-layer simulations. *Journal of Computational Physics*, 140:233–258.

Moin, P. and Moser, R. D. (1989). Characteristic-eddy decomposition of turbulence in a channel. *Journal of Fluid Mechanics*, 200:471–509.

Moser, R. D., Kim, K., and Mansour, N. N. (1990). DNS of Turbulent Channel Flow up to $Re_\tau = 590$. *Physics of Fluids*, 11:943–945.

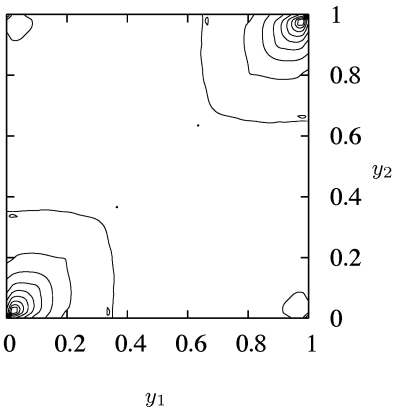

Figure 1: Real part of $R_{uu}(y_1, y_2, k_z, 0)$, $m_z = 5$

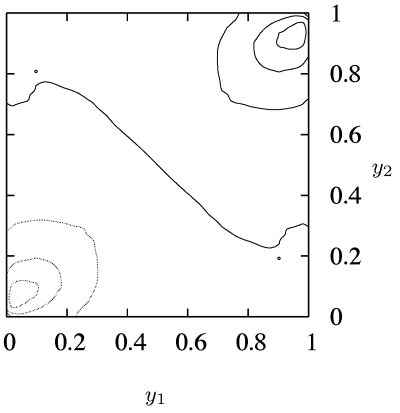

Figure 2: Real part of $R_{uv}(y_1, y_2, k_z, 0)$, $m_z = 5$. Grey contours denote negative values

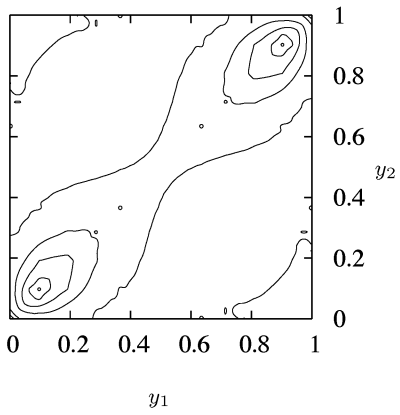

Figure 3: Real part of $R_{vv}(y_1, y_2, k_z, 0)$, $m_z = 5$

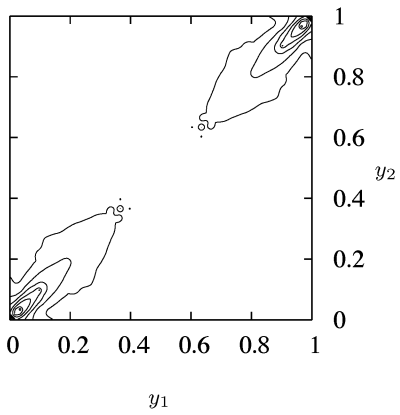

Figure 4: Real part of $R_{uv}(y_1, y_2, k_z, 0)$, $m_z = 5$

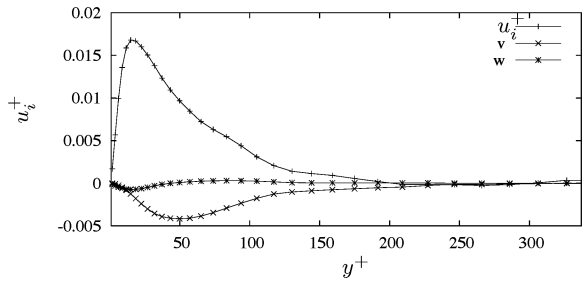

Figure 5: Real part of the first eigenvector of $R_{ij}(y_1, y_2, k_z, 0)$, $m_z = 5$. u,v and w components

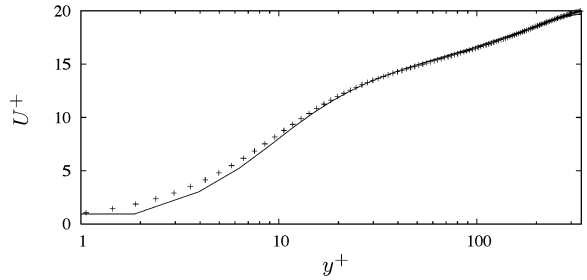

Figure 6: Mean stream-wise velocity. - LES; Symbols: DNS, Moser et al. (1990)

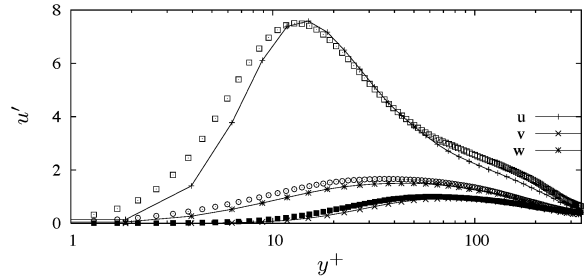

Figure 7: Stream-wise, wall-normal and span-wise turbulence intensities. - LES; Symbols: DNS, Moser et al. (1990)

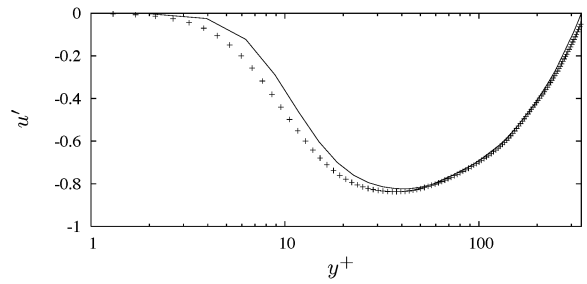

Figure 8: Reynolds stresses. - LES; Symbols: DNS, Moser et al. (1990)

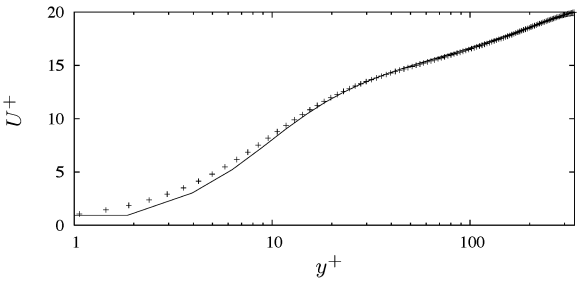

Figure 9: Mean stream-wise velocity. Inflow-outflow run. - LES; Symbols: DNS, Moser et al. (1990)

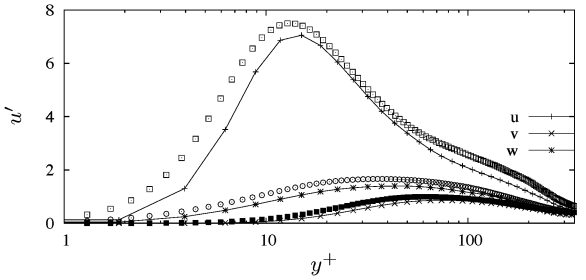

Figure 10: Stream-wise, wall-normal and span-wise turbulence intensities. Inflow outflow run. - LES; Symbols: DNS, Moser et al. (1990)

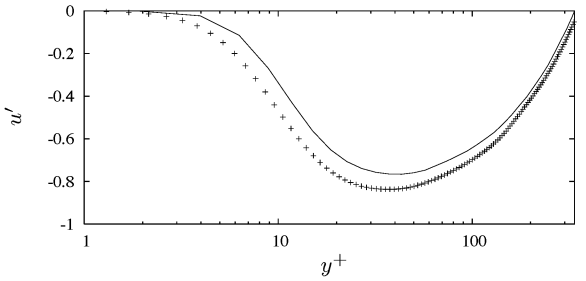

Figure 11: Stream-wise, wall-normal and span-wise turbulence intensities. Inflow outflow run. - LES; Symbols: DNS, Moser et al. (1990)